

R. WŁODARCZYK*

POROUS CARBON MATERIALS FOR ELEMENTS IN LOW-TEMPERATURE FUEL CELLS**POROWATE MATERIAŁY WĘGLOWE STOSOWANE DO BUDOWY ELEMENTÓW W NISKOTEMPERATUROWYCH OGNIWACH PALIWOWYCH**

The porosity, distribution of pores, shape of pores and specific surface area of carbon materials were investigated. The study of sintered graphite and commercial carbon materials used in low-temperature fuel cells (Graphite Grade FU, Toray Teflon Treated) was compared. The study covered measurements of density, microstructural examinations and wettability (contact angle) of carbon materials. The main criterion adopted for choosing a particular material for components of fuel cells is their corrosion resistance under operating conditions of hydrogen fuel cells. In order to determine resistance to corrosion in the environment of operation of fuel cells, potentiokinetic curves were registered for synthetic solution $0.1\text{M H}_2\text{SO}_4 + 2\text{ ppmF}^-$ at 80°C .

Keywords: fuel cell, bipolar plates, corrosion resistance, porosity, carbon materials

W ramach niniejszej pracy badano porowatość, rozkład porów, kształt porów i powierzchnia właściwa materiałów węglowych. Badania dotyczyły spiekane grafitu i materiałów komercyjnych wykorzystywanych do budowy ogniwo niskotemperaturowych (Graphite Grade FU, Toray Teflon Treated).

W pracy zamieszczono wyniki badań dotyczące pomiarów gęstości, mikrostruktury i zwilżalności (kąt zwilżania) materiałów węglowych. Głównym kryterium wskazującym wybór konkretnego materiału do elementów ogniwo paliwowych jest ich odporność na korozję w warunkach pracy wodoroowego ogniwa paliwowego. W celu określenia odporności na korozję w środowisku pracy ogniwo paliwowych, zarejestrowano krzywe potentiokinetic w roztworze $0,1\text{ M H}_2\text{SO}_4 + 2\text{ ppmF}^-$ w 80°C .

1. Introduction

Proton exchange membrane fuel cells (PEMFCs) belongs to the low-temperature generator of electricity and heat. Most of fuel cells designed for electricity production make use of hydrogen oxidation on the anode and oxygen reduction on the cathode. Individual cells contain two electrodes separated by the membrane, diffusion layers and bipolar plates. Electrolytic membrane, electrodes and diffusion layers are located between bipolar plates, with channels for equal distribution of fuel and oxidant. Most of the elements in the cell are made of carbon-based materials. The significant part of the PEMFC stack is the bipolar plates, which account for about 80% of total weight [1] and 45% of generator cost [2]. The requirements for a bipolar plate material are good thermal and electric conductivity, chemical stability in anodic and cathodic environmental, lightweight, inexpensive and easily manufactured [3,16]. By many authors, the ideal material for bipolar plates is graphite despite its brittleness and lack of mechanical strength or composites based on graphite [4-6].

Another carbon material was used for diffusion layers in PEMFC. Gas diffusion layers (GDL) support the effective diffusivity of gases through the layer [7, 8]. For the proper

functioning of GDL, it is typically coated with non-wetting polymer polytetra-fluoroethylene (PTFE) to create hydrophobic surface and pores of appropriate size [9]. The type of pores provide proper transport media in the cell. The influence of porosity on the efficiency components of the fuel cell is dealt by Lee et al. [10]. In this work, they prepared different porous gas diffusion layers by applying. Also, there are information about finding the optimum porosity and distribution of pore size in GDL. A novel composite bipolar plates based graphite were examined by Kuan and al. [11]. The porosity of the composites increased as the graphite size is decreased from $1000\text{-}177\text{ }\mu\text{m}$. The graphite composites with vinyl ester resin show good corrosion resistance and excellent flame retardance.

By IUPAC (*International Union Pure and Applied Chemistry*) the porous material can be distinguished in the field of micro pores (diameter $<0.002\text{ }\mu\text{m}$), mesopores (diameter $0.002\text{-}0.050\text{ }\mu\text{m}$) and macro pores (diameter $>0.050\text{ }\mu\text{m}$) [12]. Micro pores and mesopores determine the size of the inner surface and have an important role in adsorption processes. Macro pores act as transport routes for access to smaller pores (transport pores). The next important factor, in addition to pore size, is their shape. The pores can take the form of spherical bubbles, narrow slits, rods [13]. They can be open or closed.

* CZESTOCHOWA UNIVERSITY OF TECHNOLOGY, DEPARTMENT OF ENERGY ENGINEERING, FACULTY OF ENVIRONMENTAL ENGINEERING AND BIOTECHNOLOGY, 19 ARMII KRAJOWEJ AV., 42-200 CZĘSTOCHOWA, POLAND

It is also important the dimensional distribution of pores in the material. The pores shape is illustrated in Fig. 1a.

Knowledge of the distribution and shape of the pores allows for a variety of application (see Fig. 1b). Following the prospect of the use of materials on elements of fuel cells, information on the structure and size of pores, channels, over two discontinuities, are extremely important. Furthermore, knowledge of the nature of the porous material allows for a various possibilities of using materials for diffusion layers, porous membranes, bipolar plates [14].

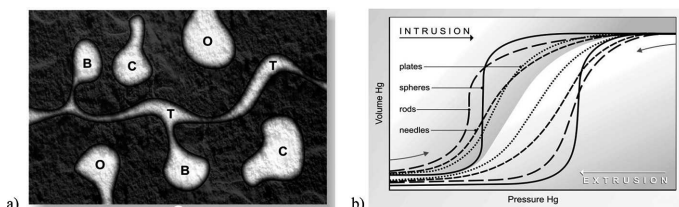


Fig. 1. a) The pore shape diagram; *O* - open; *B* - bottle; *C* - closed; *T* - transport; b) Characteristic hysteresis loops for pores formed within aggregates [15]

2. Experimental Part

The graphite powder Graphite FC manufactured by Schunk Kohlenstofftechnik GmbH (Germany) was investigated. The graphite powder was compacted with the load of 200 MPa by axial compression, and then sintered at the temperature of 1250°C for 30 minutes in vacuum. In order to compare the properties of sintered graphite materials used in the construction of a low-temperature fuel cell, commercial Graphite Grade FU 4369, and carbon paper Toray Teflon Treated were tested.

3. Results and Discussion

The samples were subjected to structural testing by means of an Axiovert optical microscope. Hardness tests for the carbon materials were carried out by means of Rockwell method.

The density and hardness of carbon materials were depicted in Table 1.

TABLE 1
Properties of carbon materials

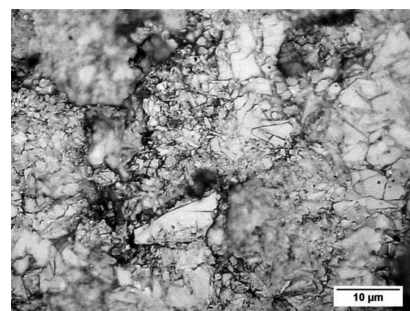
Material	Density [g cm^{-3}]	Hardness Rockwell
Sintered Graphite	1.97	97 HRF
Graphite Grade FU	1.87	100 HRB
Toray Teflon Treated	0.67	Not tested

The porosity were carried out using mercury porosimeter PoroMaster 33. Properties of the sinters are presented in Table 2.

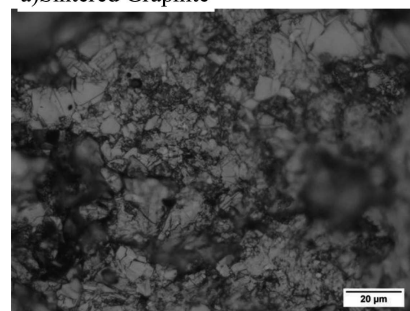
TABLE 2
Porosity and contact angle of carbon materials

Material	Porosity [%]	Contact angle [deg]
Sintered Graphite	10.73	102 \pm 0.37
Graphite Grade FU	0.93	70 \pm 0.15
Toray Teflon Treated	63.0	110 \pm 0.45

Microstructure analysis revealed visible, irregular pores which were unevenly distributed throughout the material (Fig. 2).



a) Sintered Graphite



b) Graphite Grade FU



c) Toray Teflon Toray

Fig. 2. Microstructure of the carbon materials, magnitude 500x

The hysteresis of mercury intrusion and extrusion in carbon materials is illustrated in Fig. 3. Figure shows a typical curves (volume vs. pressure curve) of a porous material with a hysteresis loop that is typical for spherical pores (Sintered Graphite) [15, 16-18]. The curves obtained for Toray Teflon and Graphite Grade, indicates that the pore shape are plate.

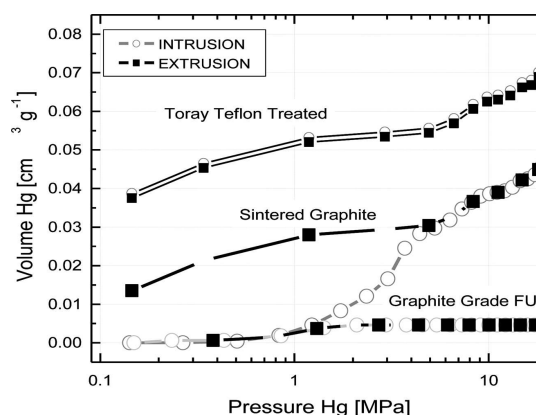


Fig. 3. Hysteresis of mercury intrusion/extrusion in carbon materials

Distribution of pores in examined materials is observed in Fig. 4. The Graphite Grade FU had a monomodal pore size distribution varying in the range of pore size 0.009-0.013 μm and porosity 0.93%. For Toray Teflon Treated and Sintered Graphite the distribution of pores is a heterogeneous form. In the case of a heterogeneous pore volume distribution curve for interpretation of the description of the actual structure of the pores inside the particles is difficult. Most of the larger pores can be, for example, on the surface of the carbon particles or between micro particles while the narrower pores may be within the grain, being an extension of the wider pores. The pores size of Sintered Graphite and Toray Teflon Treated are respectively 0.032-0.046 μm ; 0.05-0.787 μm and 0.01-10 μm . The consequence of the high porosity of the material is its high active surface (Fig. 5). Toray Teflon Treated with 63.0% porosity shows the specific surface area about 2.64 $\text{cm}^2 \text{g}^{-1}$.

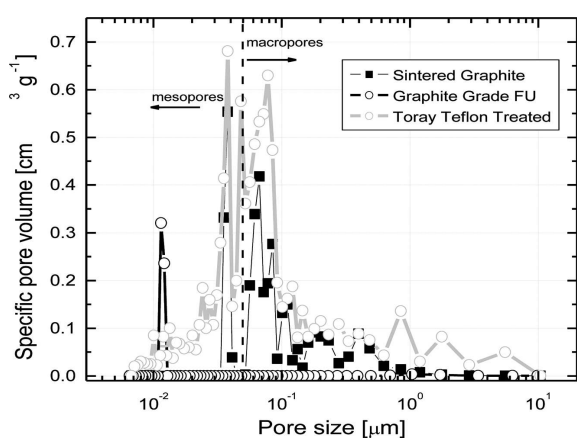


Fig. 4. Distribution of pores in carbon materials

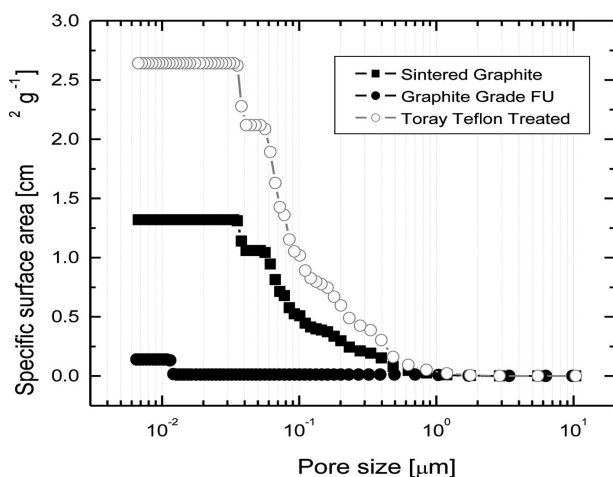
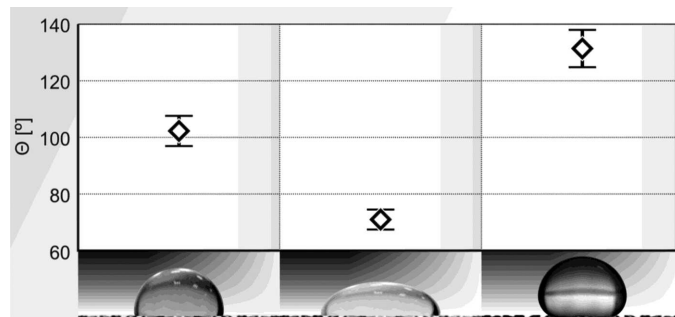


Fig. 5. Specific surface areas of carbon materials

Surface properties of materials such as porosity, surface roughness, are closely affect of wettability. The analysis of wettability was carried out through evaluation of Θ angle. Sintered Graphite and Toray Teflon Treated belong to a group of hydrophobic materials (Table 2, Fig. 6) (Θ angle above 90°).

Corrosion resistance of materials depend on wettability. The presence of water on the material surface initiates the corrosion processes. Fig. 7. presents potentiokinetic curves recorded for carbon materials in solution of 0.1 mol dm^{-3}

$\text{H}_2\text{SO}_4 + 2 \text{ ppm F}^-$ (PEMFC environmental) at 80°C . It was observed on the basis of the course of potentiokinetic curves that the carbon materials do not show a passive range (after exceeding of corrosion potential, solubilization of the material occurs with the rate increasing with rise in the level of potential).



a) Sintered Graphite b) Graphite Grade FU c) Toray Teflon T.

Fig. 6. Contact angle evaluated for carbon materials

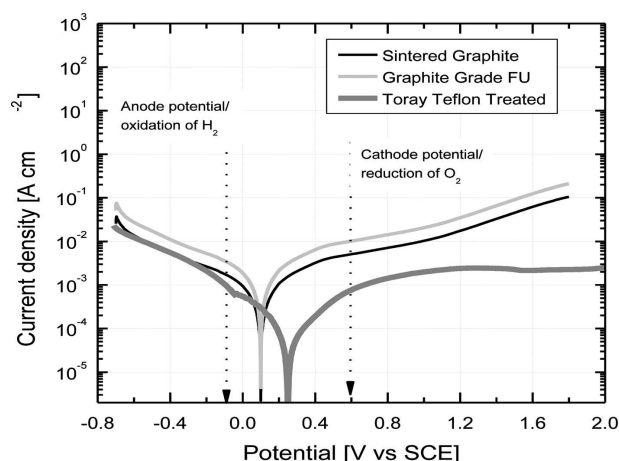


Fig. 7. Potentiokinetic curves recorded for carbon materials

TABLE 3

Corrosion parameters for the carbon materials

Material	E_{corr} [V]	i_{corr} [A cm^{-2}]
Sintered Graphite	0.098	$1,663 \cdot 10^{-4}$
Graphite Grade FU	0.092	$0,012 \cdot 10^{-1}$
Toray Teflon Treated	0.248	$1,404 \cdot 10^{-4}$

Polarization curves were used for determination and evaluation of corrosion parameters: corrosion potential (E_{corr}) [V], current density (i_{corr}) [A cm^{-2}] (Table 3). The highest corrosion resistance (the low value of current density) is observed for Sintered Graphite and Toray Teflon Treated.

4. Conclusion

In Figure 8 summarizes the results of the study. It demonstrated the relationship between the wettability of the material and a corrosion-resistant porous material. The porosity of less than 10% gives a material wetttable. The increase in porosity of the material changes the surface properties and provides a hydrophobic material.

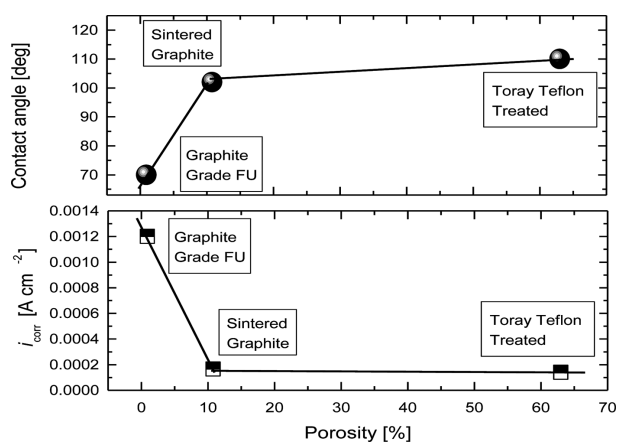


Fig. 8. Effect of porosity onto contact angle and corrosion resistance of carbon materials

Effect on the corrosion resistance of the material structure, chemical composition, corrosive environment (a kind of solution, temperature, mixing) were examined. Taking into account the porosity of the material, the general conclusion can be drawn that the value of in excess of 10% ensures high resistance to corrosion in the tested conditions. Positive effect on the corrosion resistance is also a property of repulsion of drops of the solution (hydrophobicity).

REFERENCES

- [1] A. Hermann, T. Chaudhuri, P. Spagnol, *Int. J. Hydrogen Energy* **30**, 1297 (2005).
- [2] H. Tsuchiya, O. Kobayashi, *Int. J. Hydrogen Energy* **29**, 985 (2004).
- [3] H. Tawfik, Y. Hung, D. Mahajan, *J. Power Sources* **163**, 755 (2007).
- [4] J.W. Lim, D.G. Lee, *Int. J. Hydrogen Energy* **37**, 12504 (2012).
- [5] J.W. Lim, D.G. Lee, *Composite Structures* **95**, 557 (2013).
- [6] H.N. Yu, Y.W. Lim, J.D. Suh, D.G. Lee, *J. Power Sources* **196**, 9868 (2011).
- [7] J. Khazaei, M. Ghazikhani, *Heat Mass Transfer* **48**, 799 (2012).
- [8] M.M. Bruno, H.R. Corti, J. Balach, N.G. Cotella, C.A. Barbero, *Funct. Mat. Lett.* **2**, 135 (2009).
- [9] J.T. Gostick, M.W. Fowler, M.A. Ioannidis, M.D. Pritzker, Y.M. Volkovich, A. Sakars, *J. Power Sources* **156**, 375 (2006).
- [10] H.-K. Lee, J.-H. Park, D.-Y. Kim, T.-H. Lee, *J. Power Sources* **131**, 200 (2004).
- [11] H.-C. Kuan, C.-C. M. Ma, K.H. Chen, S.-M. Chen, *J. Power Sources* **134**, 7 (2004).
- [12] www.iupac.org, website, 2013.
- [13] www.quantachrome.com; Pore network modeling from mercury intrusion/extrusion porosimetry, website, 2013.
- [14] R. Włodarczyk, A. Dudek, R. Kobylecki, Z. Bis, *Handbook: Corrosion Resistance*, Chapter 9: Corrosion resistance of composites based to graphite used as bipolar plates in fuel cells, Book edited by: H. Shih - INTECH, 189-212 (2012).
- [15] P.A. Webb, et al., *Analytical Methods in Fine Particle Technology*, Micromeritics Instrument Corporation, Norcross, GA (1997).
- [16] R. Włodarczyk, A. Wrońska, *Arch. Metall. and Mater.* **58**(1), 1 (2013).
- [17] R. Włodarczyk, A. Dudek, *Arch. Metall. and Mater.* **56**(3), 797 (2013).
- [18] A. Dudek, R. Włodarczyk, *Mat. Sci. Eng. C* **C33**, 434 (2013).